Synthesis, Self-Assembly, Fluorescence, and Thermosensitive Properties of Star-Shaped Amphiphilic Copolymers with Porphyrin Core

TIANBIN REN,[1,2] AN WANG,[1] WEIZHONG YUAN,[1,2] LAN LI,[1] YUE FENG[1]

[1]Institute of Nano and Bio-Polymeric Materials, School of Materials Science and Engineering, Tongji University, Shanghai 200092, People's Republic of China

[2]Key Laboratory of Advanced Civil Engineering Materials, Ministry of Education, Shanghai 200092, People's Republic of China

Received 29 December 2010; accepted 3 March 2011
DOI: 10.1002/pola.24665
Published online 28 March 2011 in Wiley Online Library (wileyonlinelibrary.com).

ABSTRACT: Star-shaped amphiphilic poly(ε-caprolactone)-*block*-poly(oligo(ethylene glycol) methyl ether methacrylate) with porphyrin core (SPPCL-*b*-POEGMA) was synthesized by combination of ring-opening polymerization (ROP) and atom transfer radical polymerization (ATRP). Star-shaped PCL with porphyrin core (SPPCL) was prepared by bulk polymerization of ε-caprolactone (CL) with tetrahydroxyethyl-terminated porphyrin initiator and tin 2-ethylexanote ($Sn(Oct)_2$) catalyst. SPPCL was converted into SPPCLBr macroinitiator with 2-bromoisobutyryl bromide. Star-shaped SPPCL-*b*-POEGMA was obtained via ATRP of oligo(ethylene glycol) methyl ether methacrylate (OEGMA). SPPCL-*b*-POEGMA can easily self-assemble into micelles in aqueous solution via dialysis method. The formation of micellar aggregates were confirmed by critical micelle formation concentration, dynamic light scattering, and transmission electron microscopy. The micelles also exhibit property of temperature-induced drug release and the lower critical solution temperature (LCST) was 60.6 °C. Furthermore, SPPCL-*b*-POEGMA micelles can reversibly swell and shrink in response to external temperature. In addition, SPPCL-*b*-POEGMA can present obvious fluorescence. Finally, the controlled drug release of copolymer micelles can be achieved by the change of temperatures. © 2011 Wiley Periodicals, Inc. J Polym Sci Part A: Polym Chem 49: 2303–2313, 2011

KEYWORDS: fluorescence; self-assembly; thermosensitive

INTRODUCTION In recent decades, considerable interests concerning with biodegradable polymers, especially the stimuli-responsive polymeric micelles prepared form amphiphilic block copolymers,[1–3] have been aroused by the development in pharmaceutical and biomedical fields. In aqueous solutions, amphiphilic copolymers can self-assemble into micelles with core-shell structure due to the aggregation of hydrophobic blocks into core and the dispersion of hydrophilic segments as corona. Some biodegradable materials, particularly polyesters have their own unique properties such as biodegradability, biocompatibility, and permeability.[4] For the core-shell type of polymeric micelles, PCL is usually adopted as hydrophobic blocks of amphiphilic copolymers, functioning as the sustained release reservoir of insoluble or unstable small molecules.[5,6] Meanwhile, outer hydrophilic chains composed of some stimuli-responsive hydrophilic polymers, render the micelles enable to exhibit not only improved water solubility and micelle stability, but also the responsiveness to external stimuli, such as temperature, light, ionic strength, or pH value.

Apart from these stimuli-responsive chains such as PNIPAM or PDEAEMA, which can provide a wide variety of polymers with functionality of responsiveness, much attempt was paid to conjugate functional molecules into polymeric structures, giving polymers more complex properties inherited from the functional moieties. Meanwhile, most of them are star-shaped polymers with multiarmed chains connected to a core via polymer linking or living polymerization. Furthermore, unlike amphiphilic polymeric micelles based on liner, grafted polymers[7–12] or dendrimers, star-shaped amphiphilic polymers[13–25] not only have well-defined and flexible architecture, controllable surface functionality, providing unique properties such as high surface reactivity and low hydrodynamic radius, but also can be easily prepared, while dendrimers suffer from complicated preparation process. With the development of polymerization techniques, the star-shaped polymers can be easily obtained by "living"/controlled polymerization techniques containing reversible addition fragmentation chain transfer polymerization (RAFT),[26–28] atom transfer radical polymerization (ATRP),[29–35] and their combinations with ring-opening polymerization (ROP).[36,37] For instance, Ranganathan et al. reported the synthesis of star copolymers in a sequential way of RAFT and ATRP,[38] whereas Yuan et al. synthesized dendritic star-block copolymers via a combination of ROP and ATRP.[39]

Correspondence to: W. Yuan (E-mail: yuanwz@tongji.edu.cn)

For thermosensitive polymers, lower critical solution temperature (LCST)[40–42] plays a key role in the applications of drug delivery, smart bioactive surfaces, and catalyst. Recently, ATRP of olig(ethylene glycol) methacrylates (OEGMA) has attracted increasing interests because of its adjustable LCST of a wide range by varying length of the ethylene oxide side chain. Besides its novel thermoresponsive solubility of PEG chains, these grafted PEG brushes provide external properties including improved solubility, biocompatibility, nontoxicity, and protein-resistance.[41,43,44] This work focuses on the stimuli responsive porphyrin-bearing star polymers, to enhance the controlled release capability of their self-assembled micelles when encapsulating guest molecules, and to improve the protein-resistance of the micelle applicable in biomedical filed.

To obtain more properties such as fluorescence,[45–47] molecule recognizability,[48–50] catalytic capability,[51,52] therapy capability,[53,54] and so forth, we conjugated porphyrin as the core of the star-shaped polymers. Compared with other star polymers with core molecules including trimethylolpropane, calixarenes, cyclodextrins and so on,[44,55–58] porphyrin, as one of the important photosensitizers, was attractive because of its promising photoelectric functions for various applications containing light-harvesting materials,[59,60] optoelectronic devices,[61] but also its novel therapeutic capacities such as tumor targeting and photodynamic therapy[62,63] for biomedical application. However, π-stacking and hydrophobic interactions in aqueous media leads to the aggregation of porhyrin and the resulting reduce in effectiveness of photodynamic effect. Herein, we report a porphyrin-conjugated polymeric micelle, in order to enhance the stability via the isolation of porphyrin molecules in PCL blocks, meanwhile to introduce fluorescence and therapeutic properties to micelle. Moreover, because of the π-stacking, prohyrin-conjugated PCL moiety may has advantage in the effectiveness of encapsulating π-contained hydrophobic molecules. Previous reports on the combination between phorphyrin and star polymers are steadily increasing. Fréchet[64,65] and Dong[66] reported a functional porphyrin-cored polymeric shell based on ROP of CL. Holder[67] and Cornelissen[68] synthesized a series of star polymers with porphyrin core using ATRP. These porphyrin-cored polymers lack water solubility and therefore are limited in further application. Mineo and Migliardo et al. reported water soluble porphyrin with PEO arms.[69,70] But little work has been conducted with thermosensitive amphiphilic copolymer as arms. Dichtel[71] et al. reported a porphyrin-cored amphiphilic diblock polymer using thermosensitive OEGMA as hydrophilic monomer. However, neither the inner chain nor the outer synthesized by ATRP are degradable. To our knowledge, there are no report on the star-shaped porphyrin-conjugated degradable and thermosensitive micelles prepared by the combination of ROP and ATRP.

In this article, novel and well-defined star-shaped amphiphilic poly(ε-caprolactone)-*block*-poly(oligo(ethylene glycol) methyl ether methacrylate) with porphyrin core (SPPCL-*b*-POEGMA) was synthesized by combination of ROP and ATRP. Namely, tetrahydroxyethyl-terminated porphyrin was sued as an imitator for the ROP of CL to prepare star-shaped poly(ε-caprolactone) with porphyrin core (SPPCL). Then, SPPCLBr macroinitiator was obtained by the reaction of SPPCL with 2-bromoisobutyryl bromide. SPPCL-*b*-POEGMA was synthesized by ATRP of OEGMA with SPPCLBr macroinitiator. In addition, the self-assembly behavior, thermosensitivity, critical micelle formation concentration (CMC), fluorescence and drug encapsulation of SPPCL-*b*-POEGMA were investigated with UV-visible spectrophotometer (UV-vis), transmission electron microscopy (TEM), and dynamic light scattering (DLS) spectrophotometer.

EXPERIMENTAL

Materials

Dichloromethane (CH_2Cl_2), dimethylformamide (DMF), and CL (Acros Organic) were purified with CaH_2 by vacuum distillation. Tin 2-ethylhexanoate ($Sn(Oct)_2$; Aldrich) and pyrrole (Aladdin-Reagent, Shanghai) was distilled under reduced pressure before use. Oligo(ethylenglyco)-methylether methacrylate (OEGMA, 300 g/mol, Aldrich) was passed through a basic alumina column to remove inhibitor before use. Copper(I) bromide (CuBr, Aldrich) was purified by acetic acid and then with methanol, stored under argon. Nitrobenzene, 4-hydroxybenzaldehyde, 2-bromoethanol, 18-crown-6, and other chemicals were obtained from Sinopharm Chemical Regent Company (SCRC) were of analytical grade and were used as received. 2-Bromoisobutyryl bromide (Aldrich) was distilled under reduced pressure.

Measurements

^1H NMR

^{1}H NMR data was obtained by a Bruker DMX-500 NMR spectrometer with $CDCl_3$ or DMSO-d_6 as solvent at room temperature. The chemical shifts were relative to tetramethsilane at $\delta = 0$ ppm for protons.

Gel Permeation Chromatography

Gel permeation chromatography (GPC) measurements were conducted on a gel permeation chromatographic system, equipped with a Waters 150C separations module and a Waters differential refractometer. The molecular weight and molecular weight distributions were calibrated against polystyrene standards, with THF as the eluent at a flow rate of 1 mL/min.

Fluorescence

Fluorescence spectra were performed on a Fluorolog-2 spectrofluorometer (Spex Industries, Edison, NJ) under the control of the dedicated SPEX DM3000F software. Fluorescence scans were performed at room temperature in the range of 500–800 nm using increment of 1 nm, and an excitation wavelength of 413 nm, which is at the absorption peak maximum for free porphyrin. Samples were dissolved in DMF at the molar concentration of 2×10^{-5} mol/L.

Optical Transmittances

The optical transmittances of polymer aqueous solution (2 mg/mL, distilled water was used as the solvent) at various temperatures were measured at a wavelength of 480 nm on

a UV-visible spectrophotometer (Lambda 35, PerkinElmer). The temperature of the sample cell was thermostatically controlled using an external superconstant temperature bath. The solutions were equilibrated for 10 min at each measuring temperature. The LCST value of the polymer solution was defined as the temperature producing a 50% decrease in optical transmittance.

TEM

Samples for TEM images were taken on a Tecnai-12 Bio-Twin transmission electron microscope (FEI, Netherlands) operating at 120 kV. A small drop from the aqueous copolymers solution (200 mg/L, filtered through a 450 nm filter) was deposited onto carbon-coated copper TEM grid. The excess of copolymer solution was wiped off with a filter paper, and the grid was dried under ambient atmosphere for 1 h.

DLS

The hydrodynamic diameter and the particle size distribution of the copolymer micelles were determined using a DLS spectrophotometer (DLS, Autosizer 4700, Malvern) equipped with an argon ion laser operating at 480 nm with a fixed scattering angle of 90°. All samples for DLS were redispersed in deionized water (1 mg/mL), sonicated for 30 s in an ice/water bath, and filtered through a 450 nm filter.

CMC

CMC of SPPCl-b-POEGMA copolymer in aqueous solution was studied on a LS55 luminescence spectrometer (Perkin-Elmer) and pyrene was used as a hydrophobic fluorescent probe. 0.2 mL of pyrene solutions (6×10^{-6} M in acetone) were added to containers, and the acetone was allowed to evaporate. Two milliliter of copolymer aqueous solutions at different concentrations were then added to the containers containing the pyrene residue. Each aqueous sample solutions with various polymer concentrations from 2×10^{-3} to 0.25 mg/mL contained the same concentration (6×10^{-7} M) of excess pyrene residue. Emission wavelength was carried out at 390 nm, and excitation spectra were recorded, ranging from 300 to 360 nm. The excitation and emission bandwidths were 5 and 5 nm, respectively. From the pyrene excitation spectra, the intensity ratio I342 was analyzed as a function of the polymer concentration. A CMC value was determined from the intersection of the tangent to the curve at the inflection with the horizontal tangent through the points at low concentration.

Synthesis of Tetrahydroxyethyl-Terminated Porphyrin

Tetrahydroxyethyl-terminated porphyrin was synthesized from 5,10,15,20-tetrakis(4-hydroxyphenyl)-21H,23H-porphyrin (THPP) (prepared according to literature[72]) and 2-bromoethanol according to the literature with minor modification.[73] Briefly, THPP (1.14 g, 1.68 mmol), K_2CO_3 (2.91 g) and 18-crown-6 (65 mg) were added to DMF (200 mL). 2-Bromoethanol (1.9 g, 15.2 mmol) was added, and the reaction system was vigorously stirred at 140 °C overnight under the argon atmosphere. Then, DMF was evaporated and the solid was dissolved in THF and extracted with deionized water. The organic layer was obtained by the addition of brine. After the evaporation of solvent, the crude product was dissolved in THF, precipitated in cold diethyl ether, filtered, and dried to yield (70%) a purple solid.

^{1}H NMR (DMSO-d_6, δ, ppm): 8.86 (s, 8H, β-pyrrole-H), 8.12 (d, 8H, *m*-Ar-H), 7.39 (d,8H, o-Ar-H), 5.01 (s, 4H,OH), 4.30 (t, 8H, OCH_2CH_2), 3.92 (t,8H, $HOCH_2$), −2.87 (s, 2H, NH).

Synthesis of SPPCL

The tetrahydroxyethyl-terminated porphyrin as a functional moiety allows the initiation for ROP of CL to afford the desired star-shaped polymers. The polymerization was carried out in the bulk using catalytic amounts of $Sn(Oct)_2$, as described in the literature.[40] A typical polymerization was carried out as follows. The dried porphyrin initiator (0.61 g, 0.71 mmol), a catalytic amount of $Sn(Oct)_2$ ([CL]/[$Sn(Oct)_2$] = 100) in dry toluene, CL (13 g, 113.6 mmol) and a dry magnetic stirring bar were added into a flame-dried polymerization tube. The mixture was bubbled with argon for 15 min to remove dissolved oxygen, and then evacuating-refilling process was repeated for three times before the polymerization was carried out at 120 °C under argon atmosphere with stirring for 24 h. After cooling down to room temperature, the reaction mixture was dissolved with CH_2Cl_2, and precipitated in methanol. The purified polymer was dried in a vacuum until constant weight to obtain green fine powders (91% yield).

$M_{n,NMR}$ = 15500, $M_{n,GPC}$ = 13900, M_w/M_n = 1.40. ^{1}H NMR ($CDCl_3$, δ, ppm): 9.16 (s, 8H, β-pyrrole-H), 8.18 (d, 8H, *m*-Ar-H), 7.35 (d, 8H, o-Ar-H), 4.65 (t, 8H, OCH_2CH_2), 4.51 (t, 8H, HO-CH_2), 4.06 (t, CH_2O in PCL), 3.65 (t, terminal CH_2O in PCL), 2.31 (t, $COCH_2$ in PCL), 1.65 (m, CH_2 in PCL), 1.38 (m, CH_2 in PCL).

Synthesis of SPPCLBr

A typical example is given below. SPPCL (5 g, 0.289 mmol) was dissolved in anhydrous CH_2Cl_2 (125 mL) under stirring. To this solution was added triethylamine (351 mg, 3.47 mmol) under argon at room temperature. The mixture was stirred and cooled to 0 °C with ice bath. Then, 2-bromoisobutyryl bromide (789 mg, 3.47 mmol) in anhydrous CH_2Cl_2 (20 mL) was added dropwise to the mixture within 30 min. The reaction was stirred for 24 h at room temperature before the solution was washed with $NaHCO_3$ aqueous solution (100 mL), and deionized water (100 mL × 2). The organic layer was dried overnight with $MgSO_4$. After evaporation of solvent, the resulting product was purified by precipitating from cold methanol.

$M_{n,NMR}$ = 16300, $M_{n,GPC}$ = 14400, M_w/M_n = 1.41. ^{1}H NMR ($CDCl_3$, δ, ppm): 9.16 (s, 8H, β-pyrrole-H), 8.18 (d, 8H, *m*-Ar-H), 7.35 (d, 8H, o-Ar-H), 4.65 (t, 8H, OCH_2CH_2), 4.51 (t, 8H, $HOCH_2$), 4.06 (t, CH_2O in PCL), 3.65 (t, terminal CH_2O in PCL), 2.31 (t, $COCH_2$ in PCL), 1.926 (s, $(CH_3)_2CBr$), 1.65 (m, CH_2 in PCL), 1.38 (m,CH_2 in PCL).

Synthesis of SPPCL-*b*-POEGMA

Star-shaped SPPCL-*b*-POEGMA were synthesized by ATRP of oligo(ethylenglyco)-methylether methacrylate (OEGMA) in anhydrous DMF with SPPCLBr as macroinitiator. In a general

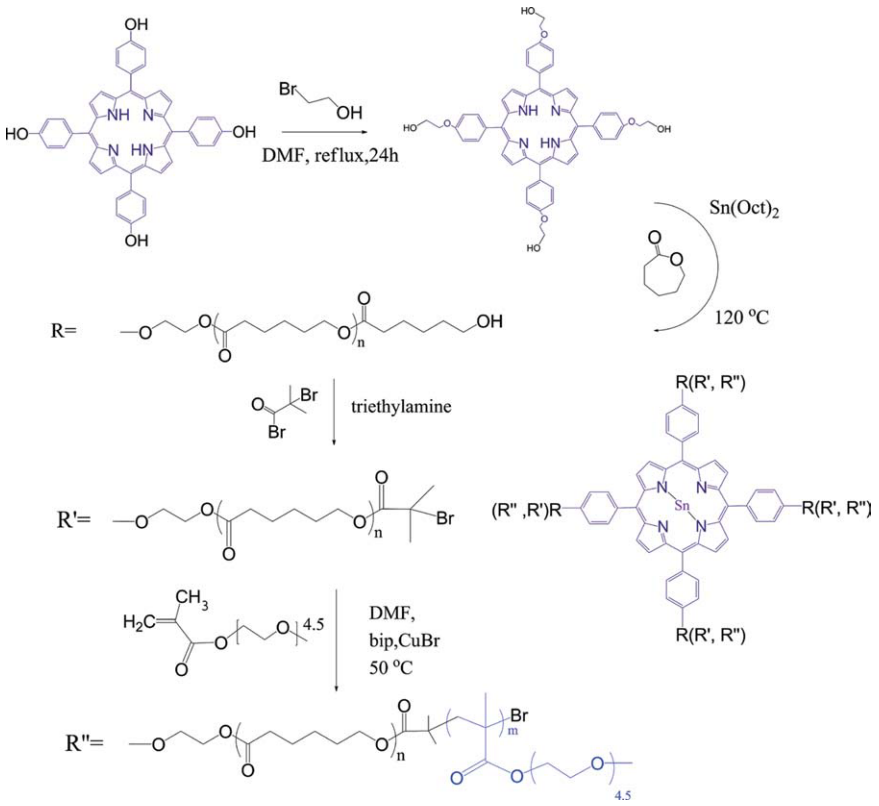

SCHEME 1 Synthesis of SPPCL-*b*-POEGMA by the combination of ROP and ATRP. [Color figure can be viewed in the online issue, which is available at wileyonlinelibrary.com.]

procedure, SPPCLBr (0.3 g, 0.068 mmol of C-Br), OEGMA (2.03 g, 6.8 mmol), bpy (46 mg, 0.3 mmol), and anhydrous DMF (3 mL) were added into a dried flask with a magnetic stirring bar. The mixture was bubbled with argon for 15 min to remove dissolved oxygen, and then degassed with three freeze-evacuate-thaw cycles after purified CuCl (21 mg, 0.15 mmol) was quickly added. The polymerization was performed at 60 °C for 120 min. Then, the experiment was stopped by exposing the catalyst to air and cooling down to 0 °C in an ice/water bath. The crude product was dissolved in THF and passed through a neutral aluminum oxide column to remove the copper catalysts and subsequently purified by dialysis against water for 72 h using a dialysis membrane with a molecular weight cut-off of 8000–12,000 (SCRC, Shanghai). The water in the resulting polymer aqueous solutions was removed by azeotropic distillation with ethanol. The crude products were dissolved in small amounts of CH_2Cl_2 and precipitated in methanol. The precipitates were filtered, dried in a vacuum oven until a constant weight.

SPPCL-*b*-POEGMA4: $M_{n,NMR} = 81300$, $M_{n,GPC} = 67000$, $M_w/M_n = 1.34$. ^{1}H NMR ($CDCl_3$, δ, ppm): 4.06 (t, CH_2O in PCL), 3.54–3.70 (CH_2CH_2O in POEGMA), 3.38 (s, terminal CH_3O of the EG block in POEGMA), 2.31 (t, $COCH_2$ in PCL), 1.53–2.01 (CH_2 on the backbone of POEGMA), 1.65 (m, CH_2 in PCL), 1.38 (m, CH_2 in PCL), 0.56–1.02 (CH_3 on the backbone of POEGMA).

Preparation of SPPCL-*b*-POEGMA Micelles

The star-shaped copolymer micelles in aqueous solution were prepared by the dialysis method. For instance, SPPCL-*b*-POEGMA4 (50 mg) was dissolved in DMF (10 mL) prior to dialysis against distilled water for 72 h using a dialysis membrane with a molecular weight cut-off of 8000–12,000 (SCRC, Shanghai). The concentration of the copolymers in aqueous solution was calculated according to the polymer weight and the volume of above micelles solution. Desired micelles concentrations can be adjusted for different characterization by diluting the micelle solution with certain amounts of deionized water.

Drug Loading and In Vitro Drug Release

Camptothecin (CPT) (4 mg) and SPPCL-*b*-POEGMA (20mg) were dissolved in 10 mL of DMF. The solution was put into a dialysis tube (MWCO: 8000–12000 g/mol, SCRC, Shanghai) and subjected to dialysis against 1000 mL of distilled water at 25 °C for 24 h. The UV absorbance of the dialysis solution was used to determine the amount of unloaded CPT (at 365 nm), which was used to calculate the encapsulation efficiency (EE%). The total amount of CPT fed initially in PBS (10 mM, pH 7.4) solution was 1.9 mg. The EE% is defined as:

$$\mathrm{EE}\% = \frac{\text{total amount of CPT} - \text{unloaded amount of CPT}}{\text{total amount of CPT}} \times 100\%$$

The EE% was found to be 47%.

RESULTS AND DISCUSSION

Synthesis of SPPCL-*b*-POEGMA

The synthesis procedure of SPPCL and SPPCL-*b*-POEGMA is illustrated in Scheme 1. The tetrahydroxyethyl-terminated

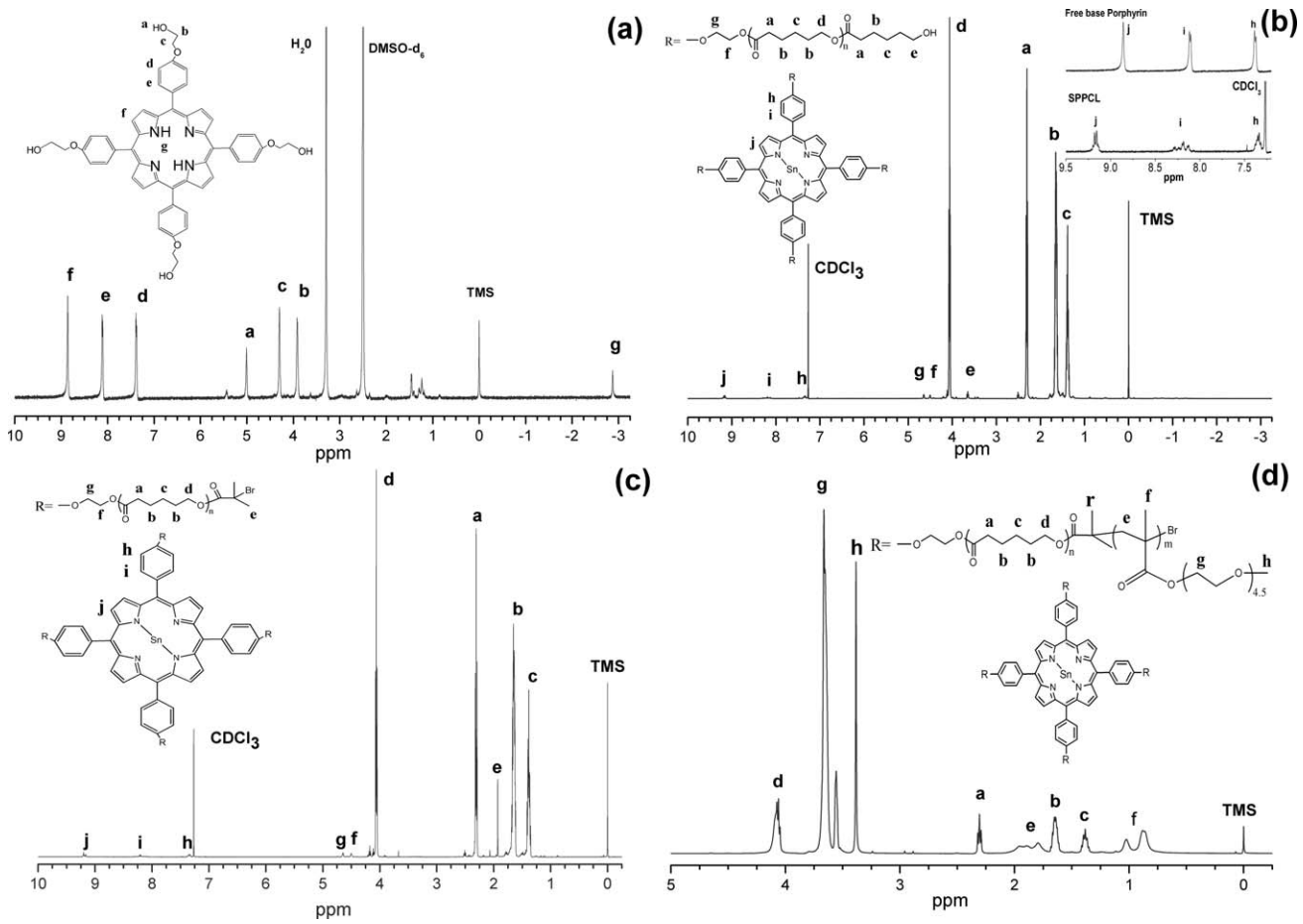

FIGURE 1 ^{1}H NMR spectra of (a) tetrahydroxyethyl-terminated porphyrin in d_6-DMSO, (b) SPPCL in $CDCl_3$, (c) SPPCLBr in $CDCl_3$, and (d) SPPCL-*b*-POEGMA in $CDCl_3$.

porphyrin was used as initiator to synthesize the SPPCL. Then, SPPCLBr macroinitiator for the subsequent ATRP of OEGMA was obtained by the bromoesterification of SPPCL with 2-bromoisobutyryl bromide. SPPCL-*b*-POEGMA was prepared from SPPCL macroinitiator and OEGMA via ATRP. Figure 1(b) shows the ^{1}H NMR spectrum of SPPCL. Compared with the spectrum of porphyrin initiator seen in Figure 1(a), not only the corresponding peaks of protons attributed to porphyrin appear, but also the major peaks attributed to protons of PCL moiety can be detected at 4.01, 2.32, 1.66, and 1.39 ppm. It demonstrates that the tetrahydroxyethyl-terminated porphyrin can initiate the ROP of CL effectively. The conversion of CL monomer was found to be 90.7%, which was calculated according to the ratio of proton peaks at 4.01 ppm and 3.65 ppm, the typical signals for —CH_2— and —CH_2OH protons on PCL moieties, respectively. The integration of proton peaks at 9.16 ppm (the β-pyrrole on prophyrin moiety) is similar to that of 3.65 ppm, indicating no PCL homopolymer formed during ROP procedure, and thus the four armed structure containing 36 repeat CL units on each arm was successfully synthesized. Moreover, proton signal of β-pyrrole appeared at 8.86 ppm [Fig. 1(a)] shifts to 9.16 ppm [Fig. 1(b)], proton signal of NH at —2.81 ppm disappeared after ROP [Fig. 1(b)], whereas the position of other protons at 8.12 and 7.39 ppm on prophyrin moiety have no significant change. This is ascribed to that complexation between tin ion and porphyrin took place which is consistent with the fact transient green appeared immediately when adding tin catalyst to mixture, and polymerization did not undertake in 72 h until the amount of tin ion was raised to 1.6 times of porphyrin. Comparing to ^{1}H NMR spectrum of SPPCL in Figure 1(b), a new peak at 1.93 ppm corresponding to the methyl protons in the bromoethyl group (—$(CH_3)_2$Br) of the macroinitiator can be detected in Figure 1(c), revealing that the terminal hydroxyl groups of PCL have reacted with 2-bromoisobutyryl bromide.

SPPCL-*b*-POEGMA copolymers were synthesized by ATRP of OEGMA with SPPCLBr as macroinitiator at 50 °C in DMF with [OEGMA]:[C-Br]:[CuBr]:[bpy] = 100:1:2.2:4.4. As shown in Figure 1(d), the peaks attributed to POEGMA block can be detected clearly. The results of ATRP of OEGMA are listed in Table 1. The molecular weight of the copolymer determined by ^{1}H NMR and GPC were all increased with the evolution of polymerization. The kinetic plot for the ATRP of OEGMA polymerization was also investigated. The ratio of the

TABLE 1 Results for ATRP of OEGMA with Star-Shaped SPPCLBr Macroinitiator

Sample	Time (min)	$M_{n,th}$[a]	$M_{n,NMR}$[b]	$M_{n,GPC}$[c]	M_w/M_n[c]	Conversion[d] (%)
SPPCL-*b*-POEGMA1	10	24,800	22,700	18,800	2.09	6.3
SPPCL-*b*-POEGMA2	20	29,100	26,200	22,100	1.68	9.9
SPPCL-*b*-POEGMA3	60	53,100	48,700	43,600	1.64	29.9
SPPCL-*b*-POEGMA4	120	86,100	81,300	67,000	1.34	57.4
SPPCL-*b*-POEGMA5	180	1,09,600	1,04,400	90,900	1.23	76.9

[a] $M_{n.th} = M_{monomer} \times ([monomer]/[C\text{-}Br]) \times 4 \times Conversion\% + M_{macroinitiator}$, [monomer]/[C-Br] =100.
[b] $M_{n,NMR}$ was determined by ^{1}H NMR spectroscopy of star-shaped copolymer.
[c] $M_{n,GPC}$ and M_w/M_n were determined by GPC analysis with polystyrene standards. THF used as eluent.
[d] Calculated from: $[(W_p\text{-}W_i)/W_m] \times 100\%$, where W_p, W_i, and W_m were the weight of the star-shaped copolymer produced, and the initial weights of the related macroinitiator and monomer, respectively.

integral areas of the methylene protons at 1.38 ppm in PCL to that of the methyl protons at 3.38 ppm on POEGMA of the resulted SPPCL-*b*-POEGMA copolymer was used to calculate the ratio of PCL and POEGMA in copolymers. As shown in Figure 2, the semilogarithmic plot of the OEGMA conversion against the reaction time had a linear increase and crossed near the zero point as expected for a controlled polymerization. The result demonstrates that the first order kinetics can be maintained under a relatively low conversion with avoiding the polymeric radical-coupling reactions, suggesting that macroinitiators retained the activity of the bromide at chain terminus during the course of polymerization, and therefore constant concentration of active species were available for subsequent reactivation. Here, $[M_0]$ and $[M_t]$ are the initial monomer concentration and the monomer concentration at time t, respectively. It can be seen from Figure 3 that $M_{n,NMR}$ were increased linearly with time, indicating that the molecular weight of the star-shaped copolymer could be manipulated by the control of monomer conversion. However, the molecular weights determined by GPC ($M_{n,GPC}$) were lower than those determined by ^{1}H NMR ($M_{n,NMR}$). This is attributed to that the star-shaped polymer has a smaller hydrodynamic volume density in comparison to the linear polystyrene as a calibration standard for GPC measurement. As shown in Table 1, the complexation of tin ion can affect not only the ROP of CL, but also the ATRP of OEGMA, leading to a relatively broad molecular weight distribution. This may be ascribed to the subsidiary reaction between Sn(II) and Cu(II). With the aid of oxidation of Sn(II), the competition from the reduction of Cu(II) may adversely affect the reverse reaction of ATRP, consequently increasing the concentration of active species and leading to a broad distribution.

The GPC traces of SPPCL, SPPCLBr, and SPPCL-*b*-POEGMA are shown in Figure 4. It can be seen that the traces are monomodal, suggesting that no mixture of star and linear polymers was formed.

UV-Vis and Fluorescence of SPPCL-*b*-POEGMA

Fluorescence of SPPCL-*b*-OEGMA was investigated by fluorescence spectroscopy. Porphyrin was used as a counterpart with the concentration of 2×10^{-5} mol/L in DMF. The

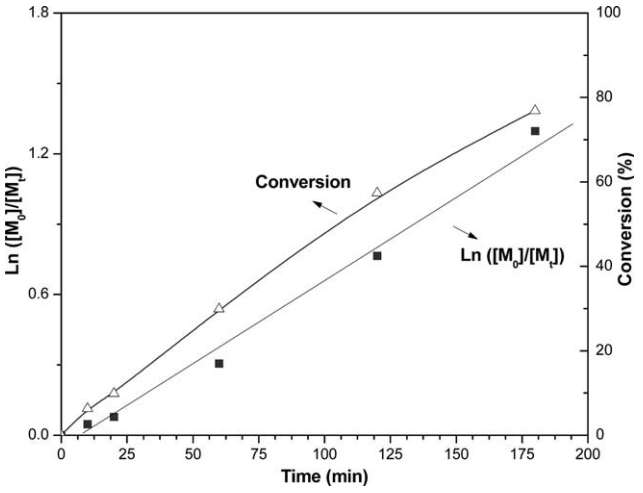

FIGURE 2 Semilogarithmic plots of monomer consumption versus time for the ATRP polymerization of OEGMA using SPPCLBr as the initiator in DMF.

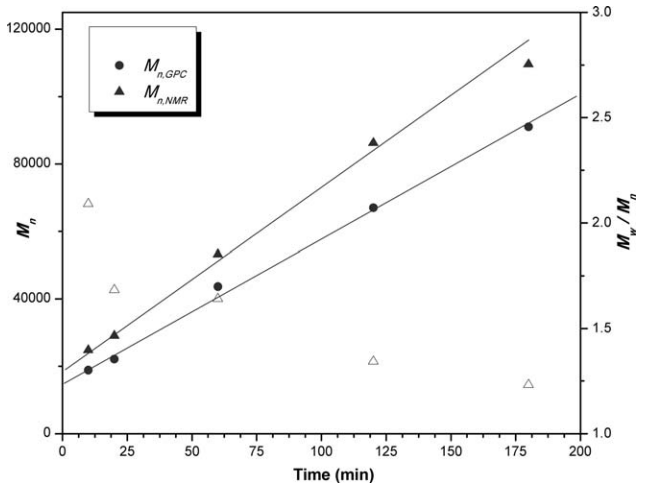

FIGURE 3 Dependence of M_n and M_w/M_n on time for ATRP of OEGMA in DMF at 50 °C.

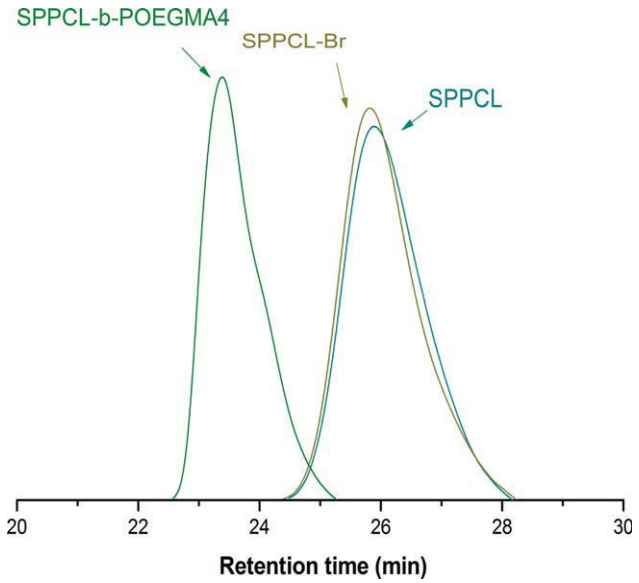

FIGURE 4 GPC traces of SPPCL, SPPCLBr, and SPPCL-*b*-POEGMA4. [Color figure can be viewed in the online issue, which is available at wileyonlinelibrary.com.]

maximum-excitation wavenumber of porphyrin was 440 nm according to the exciton spectrum. Figure 5 shows the fluorescence spectra of porphyrin, SPPCLBr, and SPPCL-*b*-POEGMA and the typical UV-vis absorption bands of porphyrins (Soret-band and Q-bands) and the difference in the Q-bands between porphyrin and polymers contained porphyrin. In the UV-vis spectra, both polymers contained porphyrin exhibit red-shifts and decreased number of Q-bands in comparison to that of porphyrin molecule. The introduction of tin ion and polymer chains induces distortion in the porphyrin plane. As a result, red-shifting in the UV-vis spectra occurred due to the lack of the expected resonance interaction, consistent with the blue shift of emission bands appeared in the fluorescence spectra. Furthermore, the insertion of tin ion was again demonstrated by the UV-vis spectra. As shown in Figure 5, concomitant with the typical Q-band of free base porphyrin disappearing at 519 nm, both the SPPCL and SPPCL-*b*-POEGMA clearly displayed tow Q-bands at 565 and 605 nm which were attributed to the tin porphyrin complex. The two spectra were closet to each other, manifesting tin ion was not replaced by Cu(II) during ATRP procedure. As a note, no significant reduction of the fluorescence intensity was found after polymerization, suggesting that SPPCL-*b*-POEGMA is capable of applications in fluorescence materials.

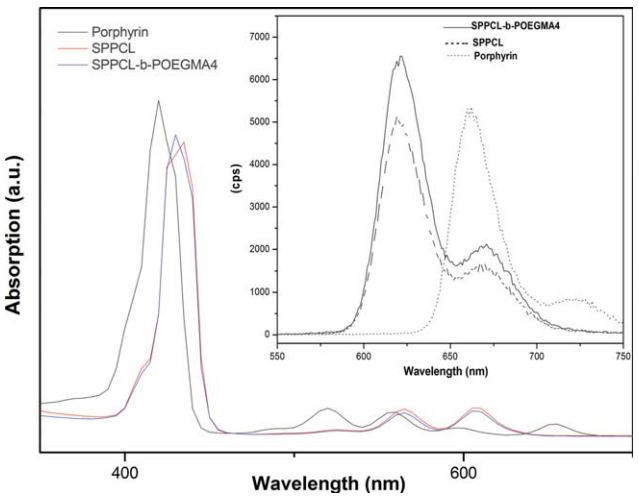

FIGURE 5 Absorbance and fluorescent spectra of porphyrin, SPPCL, and SPPCL-*b*-POEGMA4 in DMSO solution with the concentration of 2×10^{-5} mol/L. [Color figure can be viewed in the online issue, which is available at wileyonlinelibrary.com.]

Self-Assembly Behavior of SPPCL-*b*-POEGMA

The micelle formation was studied by fluorescence probe technique with use of pyrene. Excitation spectra of pyrene in the SPPCL-*b*-POEGMA solutions are shown in Figure 6. Concomitant with the increase in concentration of copolymer, there was a growing tendency of fluorescent intensity. It is worthy to note that intensity curves are closest to each other at low concentrations, however, obvious growing tendency only can be found at relatively high concentrations. This is ascribed to that pyrene preferentially aggregates into the hydrophobic core of the micelles, allowing the change of the photophysical properties. The maximum intensity at 342 nm is plotted against the logarithm of polymer concentration in Figure 8, indicating the CMC value is around 33.9 mg/L. The low degree of hydrophobic porpyrin-PCl moiety may result in such low CMC value.

TEM was used to investigate the morphology of the micelles. The micelles of SPPCL-*b*-POEGMA were prepared in aqueous solution by dialysis method at room temperature. The typical TEM image of the micelles of SPPCL-*b*-OEGMA is shown in Figure 7. It can be seen that SPPCL-*b*-POEGMA amphiphilic copolymers can self-assemble into stable and uniform spherical micelles. PCL block is hydrophobic and POEGMA block is

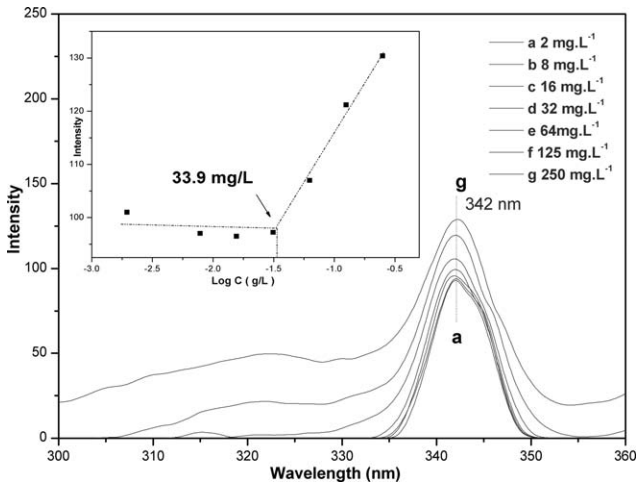

FIGURE 6 Excitation spectra of pyrene at $\lambda_{em} = 390$ nm with increasing concentrations of SPPCL-*b*-POEGMA4 copolymer and the plots of the intensity at 342 nm vs. log C.

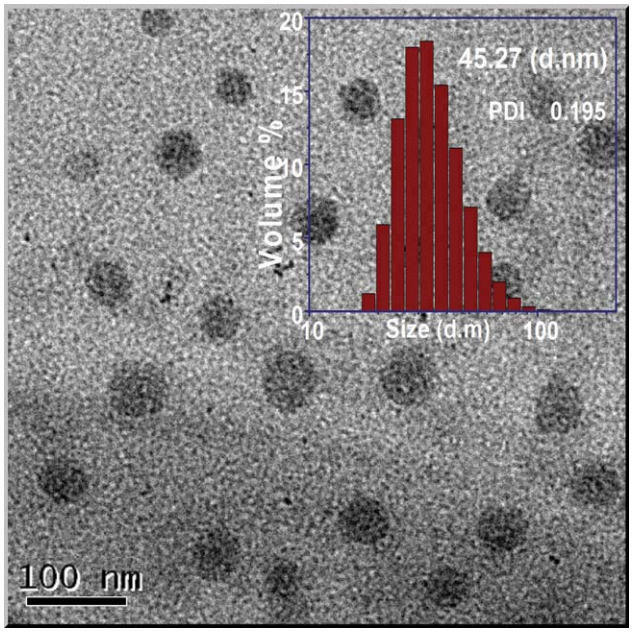

FIGURE 7 TEM image of SPPCL-*b*-POEGMA4 micelles in aqueous solution (0.2 mg/mL). [Color figure can be viewed in the online issue, which is available at wileyonlinelibrary.com.]

hydrophilic, so that this amphiphilic copolymer of SPPCL-*b*-OEGMA can self-assemble into micelles. It is reasonable that hydrophobic PCL is in the core of the micelles, whereas the hydrophilic block is in corona of the micelles. Considering the CMC value is below the concentration (200 mg/L) for TEM characterization, the formed micelle should be aggregates from individual molecule. Investigated by DLS, the 45 nm of average diameter and monomodal size distribution of the sample are consistent with the results studied by TEM.

Thermosensitivity of SPPCL-*b*-POEGMA

To investigate the thermosensitive property of SPPCL-*b*-POEGMA, the LCST was examined by the optical transmittance of a polymeric micelle aqueous solution. Figure 8 represents the curves of transmittance with the increase of temperature, revealing the temperature dependence of optical transmittance at 480 nm for the polymer aqueous solution. It can be seen that during the first step, along with the temperature increasing, the optical transmittance shows a slight increase, whereas the average diameters determined by DLS (Fig. 8) exhibit a decreased trend. These results attribute to the fact that as the temperature is raised, the hydrogen bonding interaction between the copolymers and water molecules subsequently moderates in the case of the enhanced thermal motion of water molecules. Therefore, the outer hydrophilic chains consequently shrank, which leads to a smaller diameter of micelles. However, a repulsive force due to the increased hydrophobicity of micelles causes large aggregates and an increase in optical transmittance. The optical transmittance decreases drastically with the temperature ranging from 60 °C to 62 °Cconsequently. The LCST value is found at 60.6 °C, as the temperature producing a

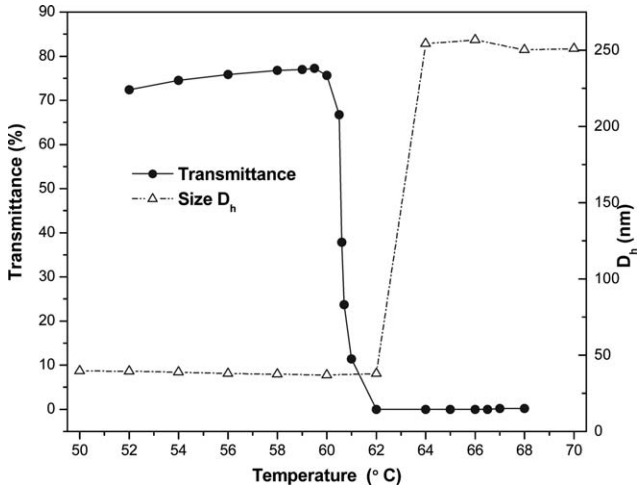

FIGURE 8 Temperature dependence of micelle size and optical transmittance at 480 nm for SPPCL-*b*-POEGMA4 aqueous solution with the concentration of 2 mg/mL.

50% decrease in optical transmittance. It can be found that above the LCST, the micelles aggregated together by the driving force of strong hydrophobic interactions, consistent with the decrease in optical transmittance and the increase in micellar size. Figure 9 indicates an enclosed photograph of the optical transmittance changes. It can be seen that the polymeric micelles dispersed in aqueous solution took on clear and turbidity dispersions respectively during a reversible cooling and heating cycles. Figure 9 also shows the curve of optical transmittance as a function of temperature for the micelle solution of SPPCL-*b*-POEGMA at the concentration of 2 mg/mL. The solutions were equilibrated for 10 min for each measuring temperature which were chosen as above and below LCST. The fluctuating value of transmittance

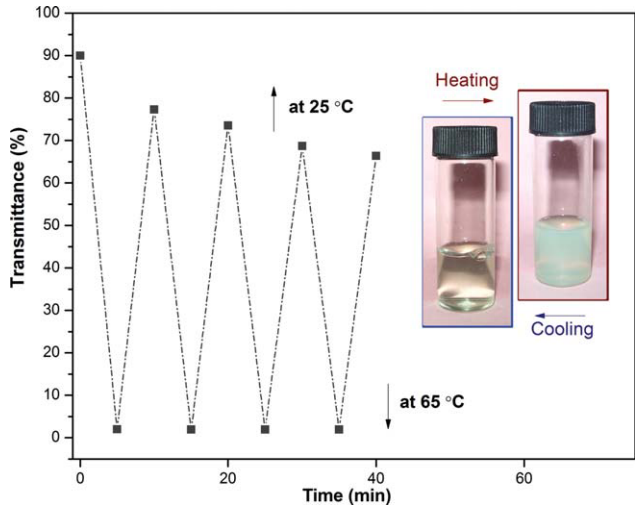

FIGURE 9 Plots of optical transmittance as a function of temperature for SPPCL-*b*-POEGMA4 aqueous solution with the concentration of 1 mg/mL (5 min for each temperature, four heating/cooling cycles between 25 and 65 °C).

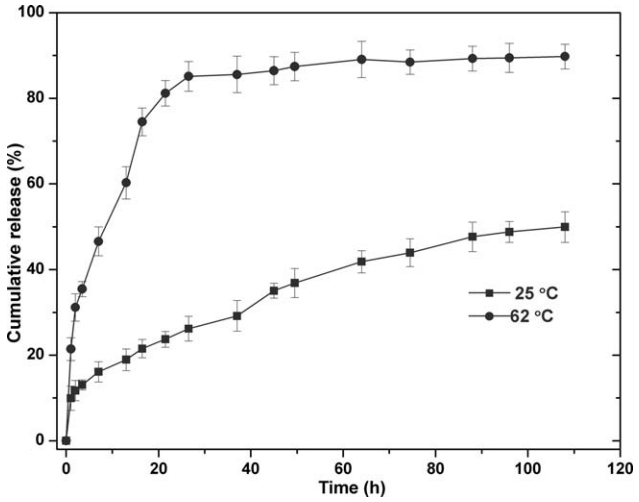

FIGURE 10 Drug release of CPT encapsulated micelle self-assembled from SPPCL-*b*-POEGMA4 copolymer.

exhibits a certain degree of cyclical characteristic of phase transition. Moreover, as demonstrated by the tendency of decrease in optical transmittance, a reasonable level of aggregation occurred during the cooling and heating cycles. The phase transition of the micelles is reversible, indicated that the micelles of SPPCL-*b*-POEGMA in aqueous solution are stable. To some extent, the obtained thermosensitive amphiphilic copolymers possess the combined properties of POEGMA, PCL and porphyrin core.

In Vitro Drug Release

The controlled release behavior of thermosensitive SPPCl-*b*-POEGMA micelles was studied in PBS (pH 7.4), as seen in Figure 10. CPT was used as a hydrophobic model drug which was physically entrapped and stabilized in the hydrophobic inner core of the micelle by hydrophobic interactions with prophyrin-PCL segment. As the temperature alterations around the LCST, significant difference in release profile can be found. At the room temperature, the highly hydrated POEGMA chain in corona of the micelles would be able to stabilize the drug-loaded hydrophobic micellar cores, allowing small amount of drug diffused out due to the concentration gradient of the inner and outer micelle. Consequently, about half of the drug still remains in the core of micelles after 108 h. Although the temperature is raised above the LCST, the hydrophobic/hydrophilic core-shell structure of the micelles is deformed. Therefore, drug release is accelerated dramatically due to temperature-induced structural changes in the micelles and 89% of the drug is released to the PBS.

CONCLUSIONS

A multifunctional micellar aggregate self-assembled from a novel porphyrin functioned star-shaped amphiphilic SPPCL-*b*-POEGMA was designed and synthesized via the combination of ROP and ATRP. Bromine-terminated SPPCL was synthesized by ROP of CL initiated with tetrahydroxyethyl-terminated porphyrin as initiator. Then, star-shaped SPPCLBr macroinitiator was obtained by the bromoesterification of SPPCL with 2-bromoisobutyryl bromide. Subsequently, SPPCLBr was used as macroinitiator to afford the ATRP of OEGMA. Investigation shows that SPPCL-*b*-POEGMA has no significant reduction in fluorescence intensity when compared with porphyrin in DMSO solution. The conformation of micellar aggregates self-assembled in aqueous solution was confirmed by fluorescence spectra, DLS and TEM. The micelles show thermo-sensitive switching behavior and exhibit the temperature induced drug release profile. Therefore, SPPCL-*b*-POEGMA has the potential applications in biomedicine and biotechnology fields, such as fluorescent tracer, dug and catalyst carrier, probe for molecular recognition, and agents for photodynamic therapy.

The authors gratefully acknowledge the financial support of the National Natural Science Foundation of China (nos. 20804029 and 30800230) and Shanghai Foundation for Development of Science and Technology (no. 0852nm03600).

REFERENCES AND NOTES

1 Kriz, J.; Masar, B.; Plestil, J.; Tuzar, Z.; Pospisil, H.; Doskocilova, D. Macromolecules 1998, 31, 41–51.

2 Stoeva, S. I.; Huo F. W.; Lee, J. S.; Mirkin, C. A. J Am Chem Soc 2005, 127, 15362–15363.

3 Jiang, X. Z.; Ge, Z. S.; Xu, J.; Liu, H.; Liu, S. Y. Biomacromolecules 2007, 8, 3184–3192.

4 Herrera, D.; Zamora, J. C.; Bello, A. Macromolecules 2005, 38, 5109–5117.

5 Quan, C. Y.; Chen, J. X.; Wang, H. Y.; Li, C.; Chang, C.; Zhang, X. Z.; Zhuo, R. X. ACS NANO 2010, 4, 4211–4219.

6 Chang, C.; Wei, H.; Quan, C. Y.; Li Y.; Wang, Z. C.; Cheng, S. X.; Zhang, X. Z.; Zhuo, R. X. J Polym Sci Part A: Polym Chem 2008, 46, 3048–3057.

7 Rosler, A.; Vandermeulen, G. W. M.; Klok, H. A. Adv Drug Deliv Rev 2001, 53, 95–108.

8 Pochan, D. J.; Chen, Z. Y.; Cui, H. G.; Hales, K.; Qi, K.; Wooley, K. L. Science 2004, 306, 94–97.

9 Gaucher, G.; Dufresne, M. H.; Sant, V. P.; Kang, N.; Maysinger, D.; Leroux, J. C. J Control Release 2005, 109, 169–188.

10 Nagasaki, Y.; Okada, T.; Scholz, C.; Iijima, M.; Kato, M.; Kataoka, K. Macromolecules 1998, 31, 1473–1479.

11 He, Y. Y.; Li, Z. B.; Simone, P.; Lodge, T. P. J Am Chem Soc 2006, 128, 2745–2750.

12 Lee, S. C.; Chang, Y. K.; Yoon, J. S.; Kim, C. H.; Kwon, I. C.; Kim, Y. H.; Jeong, S. Y. Macromolecules 1999, 32, 1847–1852.

13 Wang, F.; Bronich, T. K.; Kabanov, A. V.; Rauh, R. D.; Roovers, J. Bioconjugate Chem 2005, 16, 397–405.

14 Yang, H.; Morris, J. J.; Lopina, S. T. J Colloid Interf Sci 2004, 273, 148–154.

15 Wei, H.; Zhang, X. Z.; Cheng, C.; Cheng, S. X.; Zhuo, R. X. Biomaterials 2007, 28, 99–107.

16 He, E.; Ravi, P.; Tam, K. C. Langmuir 2007, 23, 2382–2388.

17 Chang, Y.; Chen, W. C.; Sheng, Y. J.; Jiang, S. Y.; Tsao, H. K. Macromolecules 2005, 38, 6201–6209.

18 Yang, Z.; Liu, J. H.; Huang, Z. P.; Shi, W. F. Eur Polym J 2007, 43, 2298–2307.

19 Li, P. P.; Li, Z. Y.; Huang, J. L. Polymer 2007, 48, 1557–1566.

20 Leiva, A.; Quina, F. H.; Araneda, E.; Gargallo, L.; Radic, D. J Colloid Interf Sci 2007, 310, 136–143.

21 Gillies, E. R.; Jonsson, T. B.; Frechet, J. M. J. J Am Chem Soc 2004, 126, 11936–11943.

22 Li, J. B.; Ren, J.; Cao, Y.; Yuan, W. Z. Polymer 2010, 51, 1301–1310.

23 Aoi, K.; Motoda, A.; Okada, M.; Imae T. Macromol Rapid Commun 1997, 18, 945–952.

24 Stapert, H. R.; Nishiyama, N.; Jiang, D. L.; Batt, C. A.; Kim, I. J Polym Sci Part A: Polym Chem 2007, 45, 3570–3579.

25 Chooi, K. W.; Gray, A. I.; Tetley, L.; Fan, Y. L.; Uchegbu, I. F. Langmuir 2010, 26, 2301–2316.

26 Pai, T. S. C.; Barner-Kowollik, C.; Davis, T. P.; Stenzel, M. H. Polymer 2004, 45, 4383–4389.

27 Mertoglu, M.; Garnier, S.; Laschewsky, A.; Skrabania, K.; Storsberg, J. Polymer 2005, 46, 7726–7740.

28 Barner, L.; Davis, T. P.; Stenzel, M. H.; Barner-Kowollik, C. Macromol Rapid Commun 2007, 28, 539–559.

29 Narrainen, A. P.; Pascual, S.; Haddleton, D. M. J Polym Sci Part A: Polym Chem 2002, 40, 439–450.

30 Liu, Q. C.; Zhao, P.; Chen, Y. M. J Polym Sci Part A: Polym Chem 2007, 45, 3330–3341.

31 Feng, X. S.; Pan, C. Y.; Wang, J. Macromol Chem Phys 2001, 202, 3403–3409.

32 Burguiere, C.; Chassenieux, C.; Charleux, B. Polymer 2003, 44, 509–518.

33 Kato, M.; Kamigaito, M.; Sawamoto, M.; Higashimura T. Macromolecules 1995, 28, 1721–1723.

34 Wang, J.S.; Matyjaszewski, K. J Am Chem Soc 1995, 117, 5614–5615.

35 Terashima, T.; Ouchi, M.; Ando, T.; Kamigaito, M.; Sawamoto, M. Macromolecules 2007, 40, 3581–3588.

36 Gou, P. F.; Zhu, W. P.; Zhu, N.; Shen, Z. Q. J Polym Sci Part A: Polym Chem 2009, 47, 2905–2916.

37 Yuan, W. Z.; Yuan, J. Y.; Zhou, M.; Pan, C. Y. J Polym Sci Part A: Polym Chem 2008, 46, 2788–2798.

38 Ranganathan, K.; Deng, R.; Kainthan, R. K.; Wu, C.; Brooks, D. E.; Kizhakkedathu, J. N. Macromolecules 2008, 41, 4226–4234.

39 Yuan, W. Z.; Yuan, J. Y.; Zheng, S. X. Hong, X. Y. Polymer 2007, 48, 2585–2594.

40 Twaites, B. R.; Alarcon, C. D.; Cunliffe, D.; Lavigne, M.; Pennadam, S.; Smith, J. R.; Gorecki, D. C.; Alexander, C. J Control Release 2004, 97, 551–566.

41 Trmcic-Cvitas, J.; Hasan, E.; Ramstedt, M.; Li, X.; Cooper, M. A.; Abell, C.; Huck, W. T. S.; Gautrot, J. E. Biomacromolecules 2009, 10, 2885–2894.

42 Jiang, X. W.; Xiong, D. A.; An, Y. L.; Zheng, P. W.; Zhang, W. Q.; Shi, L. Q. J Polym Sci Part A: Polym Chem 2007, 45, 2812–2819.

43 Ma, H. W.; Li, D. J.; Sheng, X.; Zhao, B.; Chilkoti, A. Langmuir 2006, 22, 3751–3756.

44 Lutz, J. F.; Weichenhan, K.; Akdemir, O.; Hoth, A. Macromolecules 2007, 40, 2503–2508.

45 Yang, J. S.; Swager, T. M. J Am Chem Soc 1998, 120, 11864–11873.

46 Chen, W. H.; Liaw, D. J.; Wang, K. L.; Lee, K. R.; Lai, J. Y. Polymer 2009, 50, 5211–5219.

47 Natori, I.; Natori, S.; Sekikawa, H.; Takahashi, T.; Ogino, K.; Tsuchiya, K.; Sato, H. Polymer 2010, 51, 1501–1506.

48 Zhu, L. N.; Yang, M. A.; Zhong, C.; Yang, C. L.; Qin, J. G. Polymer 2009, 50, 5422–5426.

49 Tian, Y. Q.; Shumway, B. R.; Meldrum, D. R. Chem Mater 2010, 22, 2069–2078.

50 Sanchez, J. C.; DiPasquale, A. G.; Rheingold, A. L.; Trogler, W. C. Chem Mater 2007, 19, 6459–6470.

51 Hasik, M.; Turek, W.; Nyczyk, A.; Stochmal, E.; Bernasik, A.; Sniechota, A.; Soltysek, A. Catal Lett 2009, 127, 304–311.

52 Dichtel, W. R.; Baek, K. Y.; Frechet, J. M. J.; Rietveld, I. B.; Vinogradov, S. A. J Polym Sci Part A: Polym Chem 2006, 44, 4939–4951.

53 Tian, Y. Q.; Wu, W. C.; Chen, C. Y.; Jang, S. H.; Zhang, M.; Strovas, T.; Anderson, J.; Cookson, B.; Li, Y. Z.; Meldrum, D.; Chen, W. C.; Jeni, A. K. Y. J Mater Chem 2010, 20, 1728–1736.

54 Bakleh, M. E.; Sol, V.; Estieu-Gionnet, K.; Granet, R.; Deleris, G.; Krausz, P. Tetrahedron 2009, 65, 7385–7392.

55 Zhu, W. P.; Ling, J.; Shen, Z. Q. Macromol Chem Phys 2006, 207, 844–849.

56 Ueda, J.; Kamigaito, M.; Sawamoto, M. Macromolecules 1998, 31, 6762–6768.

57 Stenzel, M. H.; Davis, T. P. J Polym Sci Part A: Polym Chem 2002, 40, 4498–4512.

58 Ohno, K.; Wong, B.; Haddleton, D. M. J Polym Sci Part A: Polym Chem 2001, 39, 2206–2214.

59 Kim, D.; Osuka, A. J Phys Chem A 2003, 107, 8791–8816.

60 Kuramochi, Y.; Sandanayaka, A. S. D.; Satake, A.; Araki, Y.; Ogawa, K.; Ito, O.; Kobuke, Y. Chem Eur J 2009, 15, 2317–2327.

61 Kobuke, Y.; Ogawa, K. Bull Chem Soc Jpn 2003, 76, 689–708.

62 Sternberg, E. D.; Dolphin, D.; Bruckner, C. Tetrahedron 1998, 54, 4151–4202.

63 Nyman, E. S.; Hynninen, P. H. J Photochem Photobiol B 2004, 73, 1–28.

64 Hecht, S.; Ihre, H.; Fréchet, J. M. J. J Am Chem Soc 1999, 121, 9239–9240.

65 Hecht, S.; Vladimirov, N.; Fréchet, J. M. J. J Am Chem Soc 2001, 123, 18–25.

66 Dai, X. H.; Dong, C. M.; Fa, H. B.; Yan, D. Y.; Wei, Y. Biomacromolecules 2006, 7, 3527–3533.

67 High, L. R. H.; Holder, S. J.; Penfold, H. V. Macromolecules 2007, 40, 7157–7165.

68 de Loos, F.; Reynhout, I. C.; Cornelissen, J. J. L. M.; Rowan, A. E.; Nolte, R. J. M. Chem Commun 2005, 1, 60–62.

69 Mineo, P.; Scamporrino E.; Vitalini, D. Macromol Rapid Commun 2002, 23, 681–687.

70 Micali, N.; Villari, V.; Mineo, P.; Vitalin, i D.; Scamporrino, E.; Crupi, V.; Majolino, D.; Migliardo, P.; Venuti, V. J Phys Chem B 2003, 10, 5095–5100.

71 Dichtel, W. R.; Baek, K. Y.; Frechet, J. M. J.; Rietveld, I. B.; Vinogradov, S. A. J Polym Sci Part A: Polym Chem 2006, 44, 4939–4951.

72 Adler, A. D.; Longo, F. R.; Finarelli, J. D.; Goldmacher, J.; Assour, J.; Korsakoff, L. J Org Chem 1967, 32, 476.

73 Vestberg, R.; Nystrom, A.; Lindgren, M.; Malmstrom, E.; Hult, A. Chem Mater 2004, 16, 2794–2804.